



UNIVERSITÀ
DEGLI STUDI
FIRENZE

FLORE

Repository istituzionale dell'Università degli Studi di Firenze

Motorcycle steering torque estimation using a simplified front assembly model: experimental validation and manoeuvrability

Questa è la Versione finale referata (Post print/Accepted manuscript) della seguente pubblicazione:

Original Citation:

Motorcycle steering torque estimation using a simplified front assembly model: experimental validation and manoeuvrability implications / Bartolozzi M.; Savino G.; Pierini M.. - In: VEHICLE SYSTEM DYNAMICS. - ISSN 0042-3114. - ELETTRONICO. - 62:(2024), pp. 759-784. [10.1080/00423114.2023.2194542]

Availability:

The webpage <https://hdl.handle.net/2158/1341511> of the repository was last updated on 2025-01-24T13:36:46Z

Published version:

DOI: 10.1080/00423114.2023.2194542

Terms of use:

Open Access

La pubblicazione è resa disponibile sotto le norme e i termini della licenza di deposito, secondo quanto stabilito dalla Policy per l'accesso aperto dell'Università degli Studi di Firenze (<https://www.sba.unifi.it/upload/policy-oa-2016-1.pdf>)

Publisher copyright claim:

Conformità alle politiche dell'editore / Compliance to publisher's policies

Questa versione della pubblicazione è conforme a quanto richiesto dalle politiche dell'editore in materia di copyright.

This version of the publication conforms to the publisher's copyright policies.

La data sopra indicata si riferisce all'ultimo aggiornamento della scheda del Repository FloRe - The above-mentioned date refers to the last update of the record in the Institutional Repository FloRe

(Article begins on next page)

Motorcycle steering torque estimation using a simplified front assembly model: experimental validation and manoeuvrability implications

Mirco Bartolozzi^a, Giovanni Savino^a, and Marco Pierini^a

^aDipartimento di Ingegneria Industriale, Università degli Studi di Firenze, Via di Santa Marta 3, 50139, Italy

ARTICLE HISTORY

Compiled March 2, 2023

ABSTRACT

Steering torque constitutes the primary motorcycle control input for the lateral dynamics; consequently, estimating it is important. Conventionally, this is done with complete motorcycle models, requiring significant identification effort. The simplified models in the literature only describe the steering torque under specific cases.

This work defined a steering assembly model with few parameters to estimate the steering torque analytically for stationary and transient manoeuvres.

The model equations followed from existing motorcycle models through simplifying hypotheses; transfer functions describing the roll response and the Lane Change Roll Index (LCRI) were obtained from these equations. Measured steering torque signals from different datasets, including diverse motorcycle classes, were used as the reference for validation.

A good agreement resulted between the estimated and measured torques, in the time and speed-acceleration domains and in terms of LCRI. When using the roll as the motorcycle response, manoeuvrability was highest at lower frequencies. The scooter was the most manoeuvrable; the sports and touring motorcycles were the least manoeuvrable at low and high frequencies, respectively. Concerning design parameters, the front-wheel spin inertia and front twist stiffness influenced manoeuvrability the most.

The model allows recreating the steering torque signal for new and pre-existing datasets using commonly measured signals; the signal can describe the riding style and the effort required. Few parameters are required, facilitating its use and reducing the computational burden, allowing its use for steering assistance systems.

KEYWORDS

Motorcycle Steering Torque; Motorcycle Dynamics; Motorcycle Manoeuvrability; Vehicle Testing, Frequency Response and Transfer Functions, Experimental Validation

1. Introduction

The rider controls the motorcycle lateral dynamics mainly through steering inputs. The steering torque input is the most effective way to control the motorcycle roll (stabilisation task) and yaw rate (path-following task); in contrast, the vehicle has a much smaller response to the upper body leaning [1]. Motorcycles, unlike cars, cannot be simulated in open-loop [2] due to their general instability. Consequently,

accurately describing the steering torque required to complete certain manoeuvres is more important and demanding.

While it is clear that control occurs primarily through the steering, there are at least two distinct aspects concerning vehicle behaviour: handling and manoeuvrability. *Handling* is relative to the response properties of a motorcycle as perceived by the human controller [3]; therefore, it depends on subjective rider perception, making a rigorous evaluation difficult. In contrast, *manoeuvrability* is objective and linked to the lateral vehicle response, for example, in terms of roll, yaw rate and corresponding derivatives, when a specific steering torque is applied. Therefore, manoeuvrability can be evaluated through different input-output responses, like the ratio of steering torque to steering angle [1] or the steering torque peak per unit of roll rate peak response [4].

Cossalter shows that the steering torque results from several pairs of contributions of similar magnitude but opposite sign [5]. This makes estimating the steering torque required to complete a certain manoeuvre challenging. Notably, Cossalter derives a straightforward expression to estimate the motorcycle manoeuvrability index called *Lane Change Roll Index* from its caster and the front wheel radius and spin inertia [6]. The expression assumes that the gyroscopic torque generated by the front wheel in the presence of roll rate constitutes the bulk of the steering torque during a lane change. The assumption proved valid, albeit mostly in peak-to-peak values, in the experimental data presented; however, no indication was given about this assumption's validity domain (e.g. concerning frequency and speed). A roll rate is only present during transients: a lane change performed with a steering torque input having a spectrum dominated by low enough frequencies could excite the motorcycle steady-state behaviour more than the transient terms, increasing the estimation error. In contrast, another work [7] defines a simplified expression for the steady-state torque contributions: the function was employed to fit and extrapolate experimental data; however, a comparison between the steering torque estimated from the motorcycle parameters and the measured one was not conducted. Moreover, the implications of the various terms from a design point of view were not discussed.

Biral [2] uses a more general approach, investigating the influence of frequency through slalom tests. A contour plot shows the influence of manoeuvre frequency and speed on the torque-to-roll transfer function. The dynamic behaviour represented is obtained through the classic Sharp's model [8]: although relatively simple, the model still requires the many parameters describing a complete motorcycle. Moreover, it considers lenticular tyres and neglects the tyre twisting torque due to camber: especially the latter influences the steering torque significantly [5], and cannot be neglected. Biral also uses a simplified version of the more sophisticated model by Lot [9] to calculate some transfer functions of interest, but their analytical form is not shown or discussed. This model requires more parameters than the one by Sharp.

This work aims to define a low-complexity model to estimate the steering torque required for both steady-state and transient manoeuvres to overcome the abovementioned limitations. This result would also allow describing low-frequency transient manoeuvres in addition to the two boundary cases. Moreover, it would also show concisely the frequency over which the transient terms become appreciable or dominant. The model should be simple so that the reduced number of parameters allows estimating the motorcycle steering torque without time-consuming and expensive measurements. A successful steering torque description would make it possible to study the implications of its analytical expression, such as investigating the influence of the motorcycle and manoeuvre parameters on the required steering torque. The article considers the case of uncombined dynamics; this assumption holds when the longitudinal acceleration is

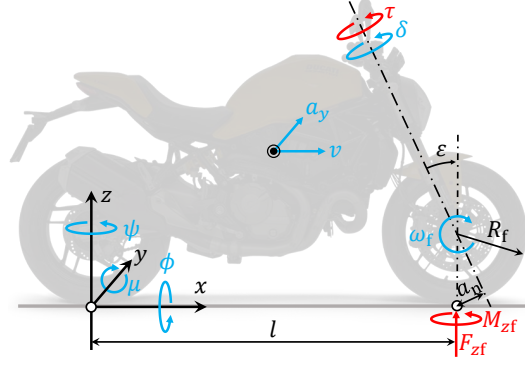


Figure 1. The signs convention and the main physical quantities considered in the article, each shown considering a positive value. The axes and the constant quantities are indicated in black, kinematic quantities are in blue, and dynamical quantities (forces and moments) are in red.

modest, especially when front braking is limited.

The paper structure follows: Section 2 describes the general methodology, including the approach used to estimate the steering torque, the instrumented motorcycle, the manoeuvres conducted and the additional dataset taken from the literature. The results, in terms of real and estimated steering torque, along with the transfer functions and maps describing manoeuvrability, are presented in Section 3; then Section 4 discusses results and their meaning. Lastly, Section 5 sums up these findings, their implications and possible extensions and applications.

2. Estimation and experimental methods

The method follows: first, the equations for describing the steering torque are derived from existing, complex dynamic models. Then, these equations are applied to different experimental datasets: one specially created through our instrumented motorcycle and then pre-existing datasets available in the literature to validate the method concerning different motorcycle classes and experimental campaigns.

2.1. Reference frame and signs convention

In this work, the ISO 8855 [10] signs convention was used: the x -axis points forwards, the z -axis upward, and consequently, the y -axis leftward. A steering torque is positive if pointing upwards. A non-tilting reference frame (Figure 1) was considered to calculate the motorcycle motion¹. The convention used justifies the signs of Equation (12): when the rider pushes (forward, positive) the right handlebar more than the left one, an anti-clockwise (positive) torque is produced.

¹The yaw rate and lateral acceleration used can be calculated from the angular velocities and accelerations measured by the IMU by applying the rotation matrices computed from the Euler Angles.

2.2. Steering torque estimation

Euler's second law of motion states, in its most general form:

$$\mathbf{M} = \frac{d\mathbf{L}}{dt} + \mathbf{v}_O \times \mathbf{p}, \quad (1)$$

where \mathbf{v}_O is the velocity of the pole O, \mathbf{M} is the resulting torque about the pole, \mathbf{L} is the system's angular momentum about that point, and \mathbf{p} is the system's linear momentum. This law is applied to the steering assembly, considering the steering axis as the pole. The steering assembly is a rigid body; therefore, its linear momentum has the same direction as its Centre of Gravity (CoG) velocity. This velocity will be approximately parallel to the velocity of the pole, as the tangential speed around the axis due to the steering angular velocity $\dot{\delta}$ is much lower than the motorcycle velocity \mathbf{v}_O . Therefore, $\mathbf{v}_O \times \mathbf{p} \approx 0$. The steering axis is a principal axis of inertia, so $\mathbf{L} = I_\delta \dot{\delta}$, where δ is the steering angle, and I_δ is the front frame moment of inertia around the steering axis. The following scalar equation is obtained:

$$\sum_{i=1}^n \tau_i = I_\delta \ddot{\delta}, \quad (2)$$

where τ_i is the i th torque component acting around the steering axis. Given that the band-pass of the rider feedback action is around 1-2 Hz [11], while higher frequencies only concern passive oscillatory stability [12, p. 284], the derivative of the angular momentum $I_\delta \dot{\delta}$ can be neglected. Therefore:

$$\sum_{i=1}^n \tau_i \approx 0. \quad (3)$$

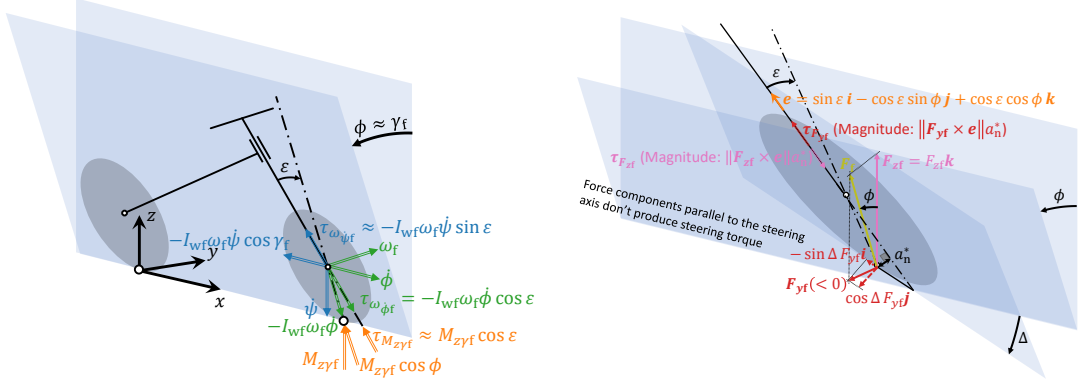
In steady-state, making the single steering torque contributions explicit gives:

$$\tau_{\text{steady}} + \tau_g + \tau_c + \tau_{F_{xf}} + \tau_{F_{yf}} + \tau_{F_{zf}} + \tau_{M_{z\gamma f}} + \tau_{\omega_{\dot{\psi}f}} = 0, \quad (4)$$

where τ_{steady} is the steady-state torque applied by the rider; τ_g and τ_c are the torques produced by the weight and centrifugal forces acting on the front frame CoG; $\tau_{F_{xf}}$ is the effect of the front tyre longitudinal force; $\tau_{F_{yf}}$ and $\tau_{F_{zf}}$ are the torques produced by the front tyre lateral and vertical forces; $\tau_{M_{z\gamma f}}$ is the steering torque due to the front tyre twisting torque; lastly, $\tau_{\omega_{\dot{\psi}f}}$ is the front wheel gyroscopic torque induced by the vehicle yaw rate $\dot{\psi}$. For this study, only the uncombined lateral dynamics is of interest, so no braking force is present on the front tyre: consequently, if the small steering torque produced by the rolling resistance when cambered is neglected, $\tau_{F_{xf}} \approx 0$ holds. Then, the steady-state torque applied by the rider balances the sum of the other contributions acting around the steering assembly:

$$\tau_{\text{steady}} = -\tau_g - \tau_c - \tau_{F_{yf}} - \tau_{F_{zf}} - \tau_{M_{z\gamma f}} - \tau_{\omega_{\dot{\psi}f}}. \quad (5)$$

For a simplified motorcycle model with lenticular wheels, neglecting the effect of the gyroscopic torque on the roll angle, the moment equilibrium in the yz plane around the front contact point shows that the sum of the weight and centrifugal forces acting on the front frame CoG passes through the front contact patch, as $\phi = -\arctan \frac{a_y}{g}$



(a) Components due to the gyroscopic effects ($\tau_{\omega_{\psi f}}$, $\tau_{\omega_{\phi f}}$) and the tyre twisting torque ($\tau_{M_{z\gamma f}}$). (b) Components due to the forces acting on the front tyre ($\tau_{F_{yf}}$ + $\tau_{F_{zf}}$).

Figure 2. Scheme of the steering torque components and their generation, shows in the case of a right-hand corner entry.

holds, where ϕ is the roll angle, a_y is the lateral acceleration, and g is the gravity acceleration. For small steering angles, this point lies in the symmetry plane of the rear frame containing the steering axis, so these two forces do not produce a resulting steering torque. These hypotheses do not hold in reality; however, τ_g and τ_c are close in value and have opposite signs in the domain of interest [5]. So, they can be neglected with minimal error.

The gyroscopic torque is equal to:

$$\tau_{\omega_{\psi f}} = -I_{wf}\omega_f\dot{\psi}\underbrace{\cos\gamma_f\sin\varepsilon}_{\approx 1}\bigg|_{\omega_f=v/R_f, \dot{\psi}=a_y/v} \approx -\frac{I_{wf}\sin\varepsilon}{R_f}a_y, \quad (6)$$

where ε is the caster angle, I_{wf} is the front wheel spin inertia, R_f is its radius and ω_f is its angular speed. In steady conditions $a_y = v\dot{\psi}$ holds, so the yaw rate can be restated as $\dot{\psi} = a_y/v$, where v is the vehicle's speed. The front tyre camber angle γ_f would make the wheel spin axis not perpendicular to the yaw rate: $\cos(\gamma_f)$ was considered ≈ 1 , leading to a modest error (5% when the angle is 18°). One can avoid this simplification without losing generality. The negative sign indicates that this torque and the lateral acceleration have opposite signs: when a_y is positive (leftward), $\tau_{\omega_{\psi f}}$ is negative (clockwise). In fact, the angular momentum of the front wheel would have a positive projection on the y -axis; as the yaw rate would be upward, the gyroscopic torque would point in the x direction, projecting on the steering axis through the $\sin\varepsilon$ term. Therefore, this torque component is aligning² and tends to reduce the steering angle. Figure 2a shows the derivation of Equation (6), with its main terms drawn in blue.

The effect of the front tyre twisting torque (First term on the right-hand side of

²One considers 'aligning' a steering torque that tends to reduce the angle between the wheel and motorcycle midplanes.

Equation (43) from Cossalter [13]) can be simplified as follows:

$$\begin{aligned}\tau_{M_{z\gamma f}} &= M_{z\gamma f} \cos \left(\underbrace{\mu}_{\approx 0} + \varepsilon \right) \underbrace{\cos \phi}_{\approx 1} \Big|_{M_{z\gamma f} = -k_{tf} F_{zf} \gamma_f} \\ &= -k_{tf} F_{zf} \gamma_f \cos \varepsilon \Big|_{\gamma_f \approx \phi = -\arctan \frac{a_y}{g} \approx -\frac{a_y}{g}} = \frac{k_{tf} F_{zf} \cos \varepsilon}{g} a_y,\end{aligned}\quad (7)$$

where k_{tf} is the normalised twist stiffness, and F_{zf} is the front tyre load: their product provides the tyre twist stiffness³, which is the tyre twisting moment $M_{z\gamma f}$ per unit of camber angle; a linear tyre behaviour is assumed. The positive sign indicates that $\tau_{M_{z\gamma f}}$ and a_y have the same sign, so the twisting torque $\tau_{M_{z\gamma f}}$ acting on the steering is misaligning. The pitch angle μ is neglected with minimal error. Figure 2a shows the derivation of Equation (7), with its main terms in orange.

Lastly, the resulting steering torque due to tyre forces $\tau_{F_{yf}} + \tau_{F_{zf}}$ (Equations (40,41) from Cossalter [13]) is considered. The following simplifying hypotheses are taken:

- The total (front and rear) resulting tyre force is parallel to the rear frame plane (and lies on it when no steering angle is present): $\tan \phi = -F_y/F_z \rightarrow F_y = F_z a_y/g$.
- By neglecting the impact of the yaw moment produced by the tyres on the front and rear partition of the total lateral force, the previous equation holds for the front tyre as well: $F_{yf} = F_{zf} a_y/g$.
- The slip angles are small. The kinematic steering angle can be calculated as $\Delta = \tan(l/R)$, where l is the wheelbase, and R is the curvature radius. Then, using $a_y = v^2/R$ and by considering small steering angles, one gets $\Delta \approx l a_y/v^2$. Additionally, under these hypotheses, $\Delta \approx \arctan(\tan \delta \cos \varepsilon / \cos \phi) \approx \delta \cos \varepsilon / \cos \phi$ [15, p. 38] and the steering angle can finally be restated as $\delta \approx l a_y \cos \phi / (v^2 \cos \varepsilon)$.

The expression reduces to:

$$\tau_{F_{yf}} + \tau_{F_{zf}} = -\frac{F_{zf} a_n \sin \varepsilon \cos \varepsilon}{g^2} a_y |a_y| + F_{zf} l a_n \sin \varepsilon \frac{a_y}{v^2} - \frac{F_{zf} l a_n \sin^2 \varepsilon}{g} \frac{a_y |a_y|}{v^2}, \quad (8)$$

where a_n is the nominal⁴ normal trail. For low enough a_y values, the $\tau_{F_{yf}} + \tau_{F_{zf}}$ component has the same sign of lateral acceleration and is misaligning. For high enough a_y values, the sign of the torque component becomes opposite to that of the lateral acceleration: the steering torque contribution becomes aligning. The second term on the right side of Equation (8) is the steering moment generated by the front tyre load due to the steering angle: $F_{zf} l a_n \sin \varepsilon a_y/v^2 \approx F_{zf} a_n \sin \Delta \sin \varepsilon$. The first and third terms on the right-hand side of Equation (8) are relative to the normal trail variation induced by the motorcycle roll and the steering angle. In the absence of a steering angle and due to the lenticular wheels assumption, the moment equilibrium in the yz plane around the vehicle CoG would cause the resulting force acting on the tyre to pass through the CoG. This fact would eliminate the steering component relative to Equation (8): the effect is analogous to the one discussed concerning the combined effect of the weight and centrifugal forces acting on the front frame. However, while the latter two produce much smaller torques having similar magnitude and opposite signs in the domain of interest [5], the torques produced by the lateral and vertical

³The tyre twist stiffness is positive, as the twisting torque is produced by the asymmetric longitudinal shear stress generated by the tyre camber and tends to self-steer the wheel [14].

⁴The one measured when the motorcycle is running straight.

tyre forces have much higher magnitudes. While still opposite in sign, their modules tend to become different for higher lateral accelerations [5] (higher roll) or for lower speeds (higher steering angle). Figure 2b shows the derivation of Equation (8). Due to the kinematic steering angle, the lateral tyre force also projects in the longitudinal direction. Due to the caster and roll angles, the unit vector \mathbf{e} of the steering axis has a component in each direction of the motorcycle frame. For each tyre force, only the component perpendicular to the steering axis produces a steering torque. The moment arm is the effective normal trail a_n^* , which is different from the nominal normal trail a_n when the motorcycle is cornering [15, p. 44].

The total steering torque applied by the rider in steady-state is, therefore:

$$\begin{aligned}
\tau_{\text{steady}}(a_y, v) &= -\tau_{M_{z\gamma f}} - \tau_{\omega_{\dot{\psi} f}} - (\tau_{F_{yf}} + \tau_{F_{zf}}) \\
&= -\frac{k_{\text{tf}} F_{zf} \cos \varepsilon}{g} a_y + \frac{I_{\text{wf}} \sin \varepsilon}{R_f} a_y + \frac{F_{zf} a_n \sin \varepsilon \cos \varepsilon}{g^2} a_y |a_y| \\
&\quad - F_{zf} l a_n \sin \varepsilon \frac{a_y}{v^2} + \frac{F_{zf} l a_n \sin^2 \varepsilon}{g} \frac{a_y |a_y|}{v^2} \\
&= -c_1 a_y + c_2 a_y |a_y| - c_3 \frac{a_y}{v^2} + c_4 \frac{a_y |a_y|}{v^2}.
\end{aligned} \tag{9}$$

The expression is analogous⁵ to that shown by Cossalter [7]. a_y^2 is replaced by $a_y |a_y|$: the torque applied by the rider is now an odd function of the lateral acceleration, allowing the description of right and left corners with the correct sign. The absolute value operation does not influence the continuity and smoothness of the function⁶. The positive coefficients c_i are determined by a limited set of motorcycle parameters; only c_1 could, in theory, be negative, but in practice, its positive portion relative to the twisting torque is significantly higher than the negative one due to the gyroscopic moment. Consequently, the steady-state torque linearly depends on the lateral acceleration (through coefficients $c_{1,3}$), with opposite signs: for small to medium lateral acceleration values, the torque applied by the rider is aligning (counter-steer). The applied torque also depends on the second power of the lateral acceleration (through coefficients $c_{2,4}$), with the same signs: this reduces the aligning torque described by the linear terms and makes the applied torque misaligning for sufficiently high lateral acceleration values. Lastly, for a given lateral acceleration, the speed influences the steering torque (through coefficients $c_{3,4}$), especially at lower speeds ($\lim_{v \rightarrow 0^+} \tau_{\text{steady}} = \infty$)⁷, while the dependency is lost at higher speeds ($\lim_{v \rightarrow +\infty} \tau_{\text{steady}} = -c_1 a_y + c_2 a_y |a_y| = \tau_{\text{steady}}(a_y)$). This fact is due to the steering angle: reaching a specific lateral acceleration at lower speeds requires a larger steering angle so that its effect on the torque becomes perceivable under a certain speed.

During transients, additional steering torques act on the steering, for example, the apparent, inertial moment $-I_\delta \ddot{\delta}$, the moment due to the steering damper (if present) and the moment generated by the component of the front tyre lateral force required to generate the yaw acceleration. Cossalter [6] investigated the lane change manoeuvre and showed that the gyroscopic torque $\tau_{\omega_{\dot{\psi} f}}$ due to the front-wheel spin velocity and the roll rate of the motorcycle is the most significant transient torque contribution.

⁵The signs are different due to the different coordinates system (SAE J670 was used in [7]).

⁶The absolute value of the independent variable a_y is always multiplied by the variable itself. $y = x|x|$ is a continuous and smooth function passing through the origin with a null slope.

⁷Notice that Equation (9) was derived assuming small steering angles, which may not hold for $v \rightarrow 0^+$.

Consequently, one can neglect all the remaining transient torques so that:

$$\tau_{\text{trans}}(v, \dot{\phi}) = -\tau_{\omega_{\dot{\phi}_f}} = I_{\text{wf}} \omega_f \dot{\phi} \underbrace{\cos \delta}_{\approx 1} \cos \varepsilon \Big|_{\omega_f = v/R_f} = \frac{I_{\text{wf}} \cos \varepsilon}{R_f} v \dot{\phi} = c_5 v \dot{\phi}, \quad (10)$$

where the angle (the steering angle δ) between the spin axis and the roll direction is assumed to be small. The gyroscopic torque and the roll rate have opposite signs: when entering a right corner ($\dot{\phi} > 0$), the torque is negative; thus, it tends to rotate the steering clockwise in the direction of the corner. This stabilising effect tends to reduce the curvature radius, leading to a higher centripetal force that reduces the roll. The rider will have to prevent it with an opposite, aligning torque. Figure 2a shows the derivation of Equation (10), with its main terms drawn in green.

Therefore, the total torque applied by the rider is estimated as:

$$\begin{aligned} \tau_{\text{est}}(a_y, v, \dot{\phi}) &= \tau_{\text{steady}_{\text{est}}}(a_y, v) + \tau_{\text{trans}_{\text{est}}}(v, \dot{\phi}) \\ &= -c_1 a_y + c_2 a_y |a_y| - c_3 \frac{a_y}{v^2} + c_4 \frac{a_y |a_y|}{v^2} + c_5 v \dot{\phi}. \end{aligned} \quad (11)$$

The previous equation can estimate the steering torque applied from the measured signals using the known motorcycle parameters. The parameters values are given for each motorcycle considered in this study in Appendix A.

2.3. Instrumented motorcycle

Figure 3 shows the sports, naked motorcycle used. A tank-mounted inertial measurement unit (XSens 680 Gi) provided the vehicle's orientation and position and their derivatives. Two strain gauges on each side of the handlebar measured the deformation due to the forces applied by the rider on the handles. A calibration procedure allowed the calculation of the applied horizontal force F ; the difference between the right and left measurement, multiplied by half the distance w_{hand} between the two knobs midpoints, provided a torque which, projected on the steering axis through the caster angle ε , constituted the measured steering torque τ_{meas} :

$$\tau_{\text{meas}} = (F_{\text{right}} - F_{\text{left}}) \frac{w_{\text{hand}}}{2} \cos \varepsilon. \quad (12)$$

The motorcycle was also equipped with outriggers⁸, allowing testing demanding conditions safely.

2.4. Experimental dataset

The dataset consisted of nineteen laps of a cone course, closed to traffic and approximately 260 m long. Each lap started with a leftward corner followed by a slalom leading to another bend to the left. A double lane change, with the two lane-changes having different geometries, completed the lap. Table 1 describes the manoeuvres. The rider avoided using the throttle and brake excessively at a lean angle (uncombined dynamics).

⁸The additional weight amounted to 25 kg (9% increase), while the roll and yaw inertia increased by around 5 kg m² and 9 kg m² respectively (around 15% and 20% increase). The rider did not notice a significant impact on the roll and yaw dynamics compared to a conventional motorcycle.



Figure 3. The instrumented motorcycle with outriggers, as used in the experiment. The positions of the inertial platform and strain gauges are shown.

Table 1. List of dataset manoeuvres.

Type	Geometry
Steady Corner	Centreline Radius 15 m
Steady Corner	Centreline Radius 12.5 m
Lane Change	3 m×14 m
Lane Change	2.75 m×5.5 m
Slalom	Cone Spacing 7 m

The maximum roll reached was 38° , during a $2.5\text{ m}\times 5.5\text{ m}$ lane change⁹, while the speed remained in the 7 m s^{-1} to 14 m s^{-1} range.

2.5. Additional dataset from the literature

In addition to the dataset above, the data from Cossalter [6] were used. The article presents the time signals relative to a 125cc scooter performing a $2.75\text{ m}\times 5.5\text{ m}$ lane change and to a heavy Touring motorcycle performing a less demanding $3\text{ m}\times 20\text{ m}$ lane change. The time signals were extracted from the figures through sampling and a cubic spline interpolation and provided data relative to additional vehicle classes compared to the motorcycle used in this study.

3. Results

3.1. Sports motorcycle

3.1.1. Steering torque estimation

Figure 4 compares the measured and estimated steering torques for our sports motorcycle during two course laps. The two signals agreed throughout the different manoeuvres; these are, starting from left: a wider steady corner (red), a slalom (green), a narrower steady corner (blue) and a double lane change (yellow). Although the rider performed the two laps slightly differently, no appreciable difference in the error was noticed. Subsection 3.1.3 will show a detailed view of the lane change section, while the reader

⁹The numbers indicate the lateral offset and the longitudinal transition distance.

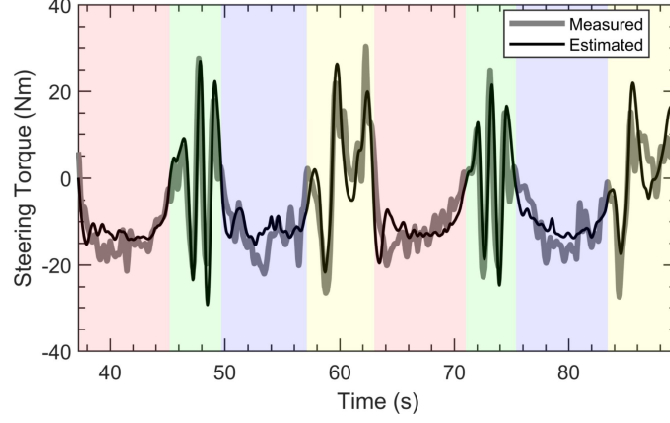


Figure 4. Comparison of the measured and estimated steering torque signals during two course laps. The manoeuvres are, starting from the left: a wider steady corner (red), a slalom (green), a narrower steady corner (blue) and a double lane change (yellow). The second lap starts at around 63 seconds.

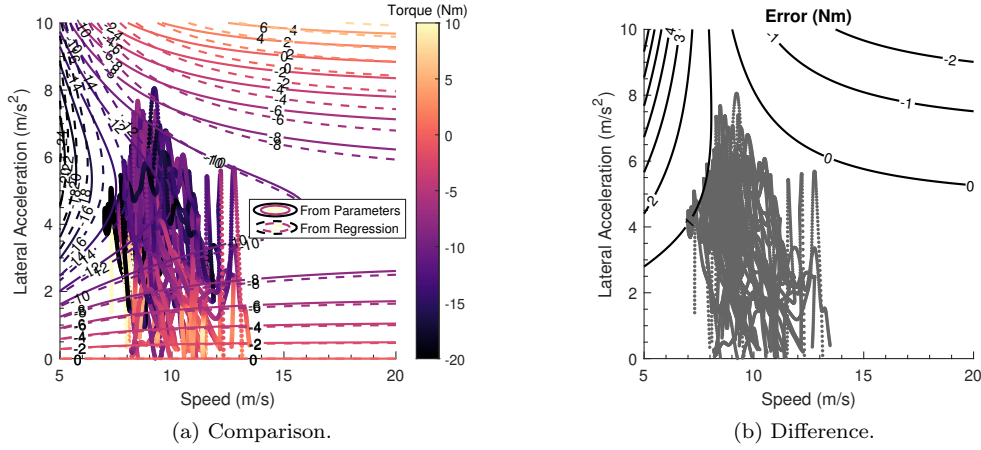


Figure 5. Steady torque maps calculated from the vehicle parameters and using the coefficients obtained from the regression. The difference between the two is shown as the ‘Error’ on the right subfigure. The dots indicate the states effectively reached by the motorcycle.

interested in cornering and slalom can find a zoom and a discussion in the Appendix B.

To further check the model’s accuracy, the comparison was repeated in the speed-acceleration domain. The estimated transient steering torque $\tau_{\text{trans_est}}$ was subtracted to the measured steering torque τ_{meas} for each time instant:

$$\tau_{\text{steady_meas}}(t) = \tau_{\text{meas}}(t) - \tau_{\text{trans_est}}(t). \quad (13)$$

The steady-state component of the measured steering torque was then fitted, as a function of speed and lateral acceleration, using Equation (9), obtaining the new coefficients $\hat{c}_{1,2,3,4}$. Only the intervals relative to the two corners were considered, starting and ending with zero roll and yaw rate. In these manoeuvres, the transient steering torque was small but present. In fact, when removed, the quality of the fit improved. Figure 5 compares the steady torque maps computed with the coefficients calculated from vehicle parameters and with coefficients from the regression. In Figure

5a, the maps showed similar behaviour in the whole speed-acceleration domain. The speed influence on the applied torque was lost at higher speeds. For a given speed, the steering torque initially increased in magnitude with the lateral acceleration, starting from zero and reaching a maximum. For low to medium lateral acceleration values, the applied torque was discordant with the lateral acceleration (counter-steering). A further increase in lateral acceleration made the steering torque decrease in magnitude, changing sign (positive-steering) for very high lateral acceleration values. For a given speed, the lateral acceleration corresponding to maximum and zero steering torque values are:

$$\frac{\partial \tau_{\text{steady}}(a_y, v)}{\partial a_y} = 0 \rightarrow a_y|_{\tau=\tau_{\text{max}}} = \frac{c_1 v^2 + c_3}{2(c_2 v^2 + c_4)}, \quad (14)$$

$$\tau_{\text{steady}} = 0 \rightarrow a_y|_{\tau=0} = \frac{c_1 v^2 + c_3}{c_2 v^2 + c_4} = 2a_y|_{\tau=\tau_{\text{max}}}. \quad (15)$$

The speed-acceleration couples reached by the motorcycle during the test are indicated by dots and spanned a wide lateral acceleration range relative to lower speed values. Given that this region was only a fraction of the possible operating conditions, Figure 5a shows the agreement between the map calculated from motorcycle parameters and that extrapolated from measured values. Figure 5b shows the difference between the two: the error was lower than 1 N m in the reached motion conditions, confirming the agreement during steady corners shown in Figure 4.

3.1.2. Manoeuvrability transfer function and sensitivity analysis

After assessing the steering torque estimation, both as a time signal and as a function of the speed and acceleration, a transfer function was derived from the model. This function would describe motorcycle manoeuvrability as a function of frequency, investigating the influence of the manoeuvre and the motorcycle parameters.

Under the assumption of negligible variation of steering angular momentum (Equation (3)), the rider balances the torques acting on the steering. Concerning manoeuvrability, the steering torque variation $\Delta\tau$ experienced at the handlebar following a roll variation $\Delta\phi$ is of interest. Equation (11) is rewritten in terms of roll, using $a_y = -g \tan \phi$, and linearised concerning small roll perturbation around the generic $\phi = \phi_0$ equilibrium condition:

$$\begin{aligned} \tau_{\text{est}}(t) &\approx \tau_{\text{steady}}|_{\phi=\phi_0} + \frac{\partial \tau_{\text{est}}}{\partial \phi}|_{\phi=\phi_0} \Delta\phi(t) \\ &:= \tau_0 + \mathcal{L}^{-1} \left(\Delta T_{\text{est}}(s) = H_{\phi \rightarrow \tau}|_{v, \phi_0}(s) \Delta\Phi(s) \right), \end{aligned} \quad (16)$$

where $H_{\phi \rightarrow \tau}(s)$ is the roll-to-torque transfer function, \mathcal{L} is the Laplace transform, s is the Laplace variable, $\Phi(s) = \mathcal{L}(\phi(t))$ and $T(s) = \mathcal{L}(\tau(t))$. The partial derivative becomes, considering that $\frac{\partial \tan x}{\partial x} = \frac{1}{\cos^2 x}$ and $\frac{\partial |f(x)|}{\partial x} = \frac{f(x)}{|f(x)|} \frac{\partial f(x)}{\partial x}$, and by grouping terms:

$$H_{\phi \rightarrow \tau}|_{v, \phi_0}(s) = \frac{g}{\cos^2 \phi_0} \left[c_1 + \frac{c_3}{v^2} - \left(c_2 + \frac{c_4}{v^2} \right) 2g |\tan \phi_0| \right] + c_5 v s. \quad (17)$$

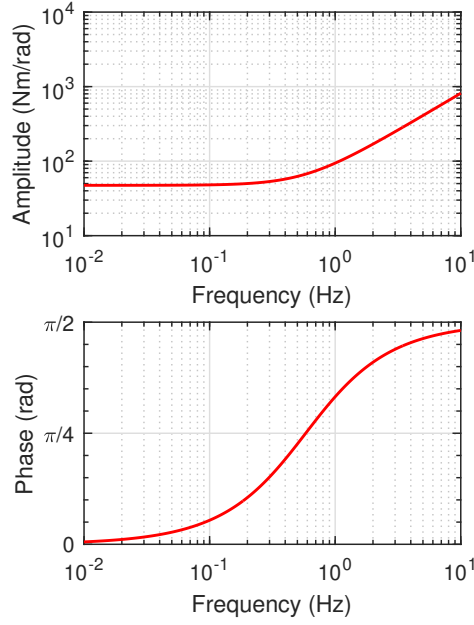


Figure 6. Amplitude and phase of the roll-to-torque transfer function ($v = 10 \text{ m s}^{-1}$, $\phi_0 = 0 \text{ rad}$).

The transfer function, computed from the motorcycle parameters, consists of a single zero. Figure 6 shows it for $v = 10 \text{ m s}^{-1}$, $\phi_0 = 0 \text{ rad}$, corresponding to the slalom manoeuvre of the dataset. When $\phi_0 = 0 \text{ rad}$, the zero is negative, as evident by Equation (17). $H_{\phi \rightarrow \tau}(s) = K(s - z)$, where K is the static gain, and z is the zero. Therefore, at lower frequencies, its amplitude is minimum and equal to the static gain, and the phase is null. Around the frequency equal to the zero, the amplitude increases, with a 20 dB per decade slope. The phase increases approximately one decade before the zero and reaches $\pi/2$ approximately one decade after. The higher the frequency, the higher the steering torque required following a roll variation. Alternatively, if one considers the torque as the input, there will be a smaller roll response for a given torque applied. Moreover, the phase increases: the steering torque perceived by the rider anticipates the motorcycle roll, or alternatively, the roll response is delayed compared to the rider input.

Figure 7 shows the influence of the manoeuvre parameters on the transfer function, with the transfer function already shown in Figure 6 plotted in red. Figure 7a shows the influence of speed: increasing the speed decreased the low-frequency amplitude, with progressively less impact. Instead, increasing the speed increased the high-frequency amplitude proportionally¹⁰. The greater the speed, the greater the influence of frequency. A speed increase lowered the frequency of the amplitude knee and shifted the phase-change to lower frequencies. Figure 7b shows the influence of the equilibrium roll angle ϕ_0 , which had no effect at higher frequencies. When increasing up to $\phi_0 = 24^\circ$, the low-frequency amplitude decreased, and the phase-change shifted to lower frequencies. This trend interrupted concerning the highest roll value ($\phi_0 = 36^\circ$, in green): the static gain crossed the zero and became negative and with higher magnitude; therefore, the amplitude at low frequencies increased. As the static gain was negative, the phase

¹⁰As evidenced by the constant vertical spacing, in the log-log plot, of lines relative to different values of the logarithmically-spaced speed.

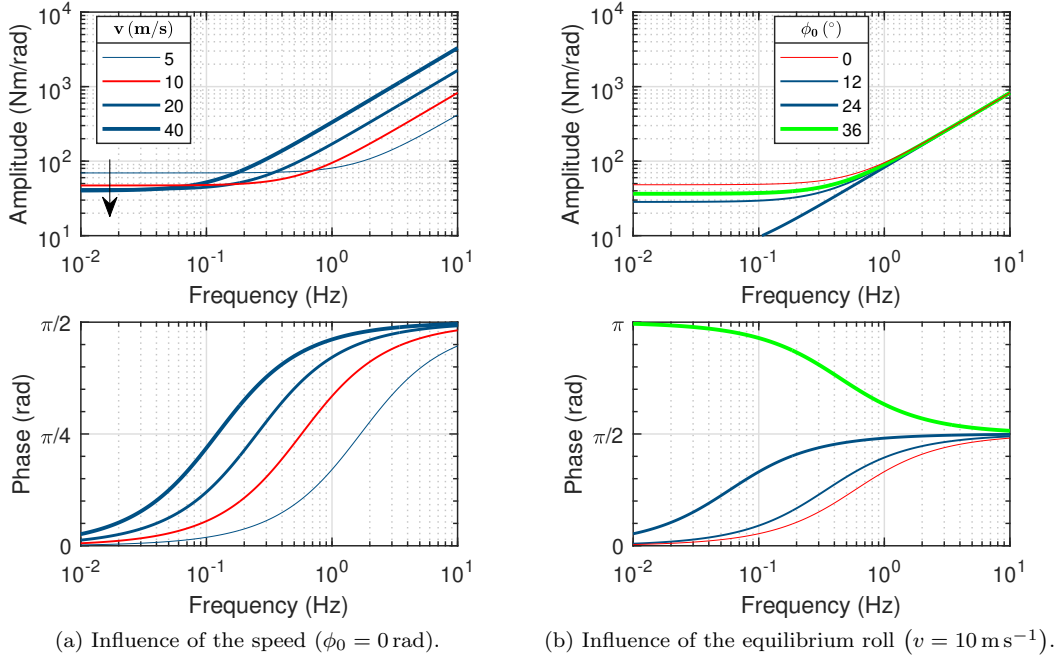


Figure 7. Influence of the manoeuvre parameters on the amplitude and phase of the roll-to-torque transfer function.

at lower frequencies became π ; the zero turned negative, so increasing the frequency decreased the phase, reaching $\pi/2$.

Figure 8 summarises these effects. In particular, Figure 8a shows the influence of the speed and equilibrium roll on the static gain: its value was high and positive at low speeds and for an upright equilibrium condition and became high and negative for high roll angle values. The static gain lost the speed dependency for high-speed values. Figure 8b shows the zero value, significantly dependent on both speed and roll. Its sign mainly depended on the equilibrium roll value and became positive for sufficiently high roll angle values. A speed increase reduced its absolute value: the change in behaviour of the transfer function between low- and high-frequency behaviour shifted to lower frequencies. Equation (14) states, in terms of lateral acceleration, the singular conditions corresponding to the sign change of the static gain and the zero.

The previous figures showed the influence of the manoeuvre parameters on the roll-to-torque transfer function. The design choices influence manoeuvrability, too: this impact can be quantified and understood by analysing the sensitivity of the transfer function to motorcycle parameters. This analysis also quantifies the effect of an error on one parameter on the estimated transfer function. Figure 9 shows this for the most significant motorcycle parameters influencing the estimated torque (Equation (11)). Figure 9a shows that increasing the front tyre normalised twist stiffness increased the static gain of the transfer function while not influencing the high-frequency amplitude. The phase-shift moved to higher frequencies. Increasing the front-wheel spin inertia (Figure 9b) decreases the transfer function amplitude at lower frequencies and increases it at higher frequencies. Moreover, increasing the inertia increased the delay between the applied torque and the resulting roll at medium frequencies. Increasing the front tyre load (Figure 9c) increases the static gain modestly, with no effect at higher frequencies. The phase reduced slightly at medium frequencies. Interestingly, the caster (Figure

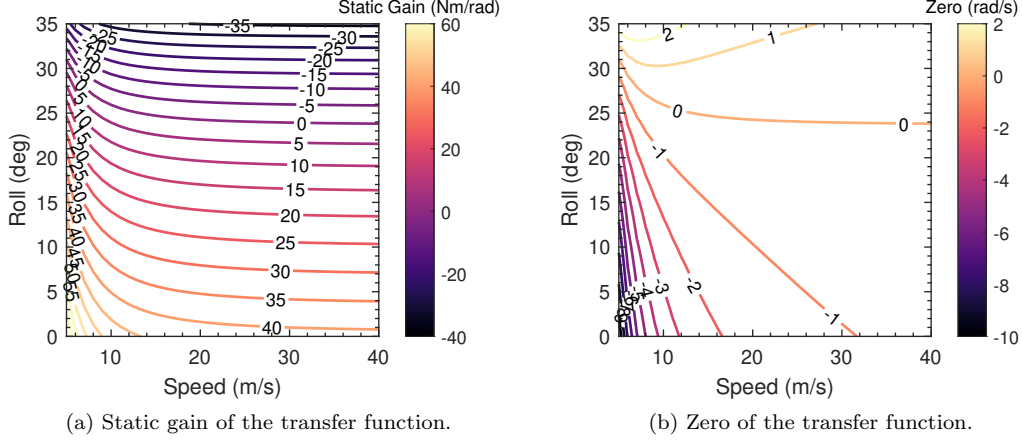


Figure 8. Influence of the manoeuvre parameters on the roll-to-torque transfer function properties.

9d) influenced the transfer function marginally¹¹. Lastly, increasing the normal trail increased the low-frequency amplitude slightly, with no effect on higher frequencies (Figure 9e). The phase was reduced at medium frequencies.

3.1.3. Lane change roll index estimation and transfer function

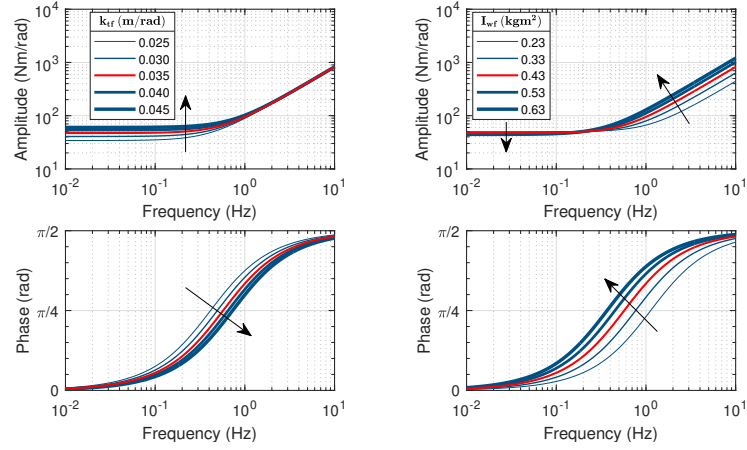
The lane change manoeuvre is commonly employed to assess vehicle behaviour and manoeuvrability. It consists of two very brief pseudo-stationary cornering phases, corresponding to the maximum roll absolute value, each preceded and followed by a demanding transient manoeuvre, in which the roll rate can reach significant values. The Lane Change Roll Index (LCRI) [6] describes the manoeuvrability during this manoeuvre as:

$$\text{LCRI} := \frac{\tau_{\text{p-p}}}{\phi_{\text{p-p}} v_{\text{avg}}}, \quad (18)$$

where ‘p-p’ stands for peak-to-peak values and ‘avg’ stands for ‘average’ through the manoeuvre. The Index evaluates the steering torque necessary to achieve a unitary roll rate response, normalised by the vehicle’s speed. It captures a comprehensive manoeuvre perspective by utilising peak-to-peak values instead of the absolute peak value, decreasing the impact of riding style on its value [6].

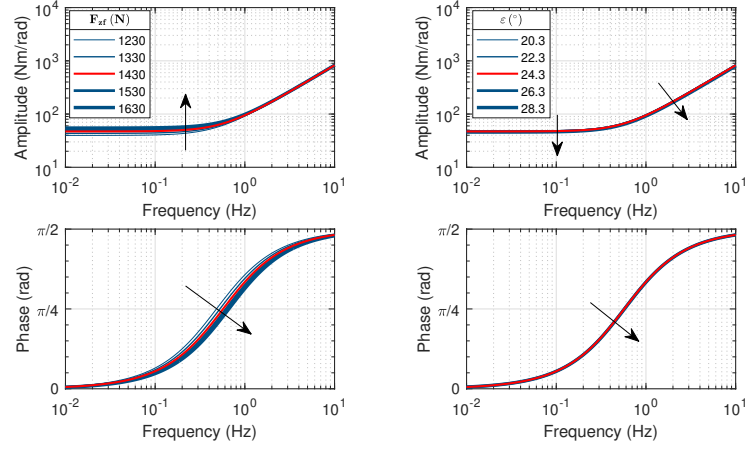
Table 2 presents the LCRI values calculated using the measured and estimated torque. Additionally, the value of the analytical, simplified expression for the LCRI by Cossalter [6], based on the transient term only, is provided. Only the 3 m×14 m lane change was considered, as the 2.75 m×5.5 m lane change exit was very close to the following corner, and the rider did not have the time to fully stabilise the bike before entering it. Moreover, the 3 m×14 m lane change runs where the motorcycle was not straight at the beginning or end of the manoeuvre, also due to limited space available, were excluded too. The measured LCRI ranged from a minimum of 1.49 N rad⁻¹ s² to a maximum of 1.91 N rad⁻¹ s², with a 1.68 N rad⁻¹ s² mean value and a 0.14 N rad⁻¹ s² standard deviation. The LCRI from the estimated torque had a 1.70 N rad⁻¹ s² mean, very close to that of the measured LCRI, and its 0.12 N rad⁻¹ s² standard deviation

¹¹This assumes that the caster changes without influencing the other parameters: in reality changing the caster requires changes to the fork offset, for example, to keep the same normal trail.



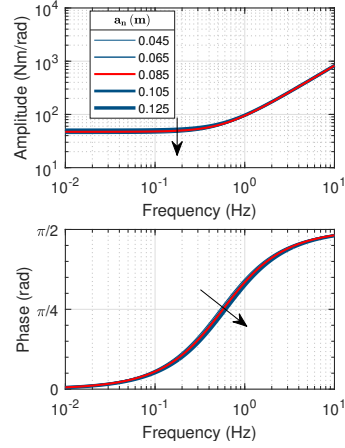
(a) Normalised front twist stiffness.

(b) Front-wheel spin inertia.



(c) Front static load.

(d) Caster angle.



(e) Normal trail.

Figure 9. Influence of the motorcycle design parameters on the amplitude and phase of the roll-to-torque transfer function. The black arrows indicate the increase in the parameter considered.

Table 2. Lane Change Roll Index calculated using the measured and the estimated steering torque for each suitable run of the 3 m×14 m lane change. The simplified formula that only considers the transient steering torque predicts a value equal to $I_{wf} \cos \varepsilon / R_f = 1.31 \text{ N rad}^{-1} \text{ s}^2$

Run Number	LCRI ($\text{N rad}^{-1} \text{ s}^2$)	
	Using τ_{meas}	Using τ_{est}
1	1.68	1.66
2	1.91	1.76
6	1.58	1.70
7	1.57	1.61
8	1.64	1.76
9	1.84	1.69
10	1.69	1.89
12	1.49	1.46
14	1.85	1.82
15	1.80	1.74
17	1.53	1.58
18	1.62	1.63
Mean	1.68	1.70
SD	0.14	0.12

indicated a metric variability similar to that obtained with the measured signal. The measured and estimated values were strongly correlated: the estimated steering torque value is lower when the measured value is lower. The LCRI calculated using the simplified expression equalled $1.31 \text{ N rad}^{-1} \text{ s}^2$, lower than the lowest measured value.

Figure 10 shows the measured and estimated torque signals, along with its components, for two Lane Change runs. Figure 10a is relative to lap six: the measured and estimated torque signals were very close in the middle section, between the two steering torque peaks. Here the motorcycle went from a small leftward roll to its maximum value to zero to change direction. Before the first peak, the estimated steering torque lagged the measured one, while after the last peak, the estimated signal did not capture¹² the oscillations of the measured one. The error on the LCRI is $0.12 \text{ N rad}^{-1} \text{ s}^2$, higher than in many other runs (Table 2). Nonetheless, there was good agreement between the estimated and the measured signal. The transient term alone underestimated the first peak and misses the dynamics of the manoeuvre exit. Figure 10b shows the signals during lap 14, where the error on the LCRI was lower ($0.03 \text{ N rad}^{-1} \text{ s}^2$). As before, the transient term underestimated the first peak while correctly reproducing the instant of each peak.

The LCRI can be expressed as the amplitude of a transfer function:

$$\text{LCRI}(s) = \left| \frac{T_{\text{est}}(s)}{\dot{\Phi}(s)v} \right| = \left| \frac{T_{\text{est}}(s)}{\Phi(s)sv} \right| = \left| \frac{H_{\phi \rightarrow \tau}(s)}{sv} \right|_{\phi_0=0} = \left| \frac{g \left(\frac{c_1}{v} + \frac{c_3}{v^3} \right) + c_5 s}{s} \right|, \quad (19)$$

where the roll equilibrium was set to zero because, during a lane change, the motorcycle rolls around its vertical configuration. The transfer function describing the LCRI is a single, negative zero with an integrator term.

During the middle section of a Lane Change manoeuvre, all the motorcycle signals have an approximately sinusoidal shape [6], with a frequency influenced by the motorcycle speed and by the lane change transition distance. Although the different signals

¹²The difference between the measured and the estimated steering torque, compared to Figure 4, is magnified by the different time scales. The same point stands for Figure 12.

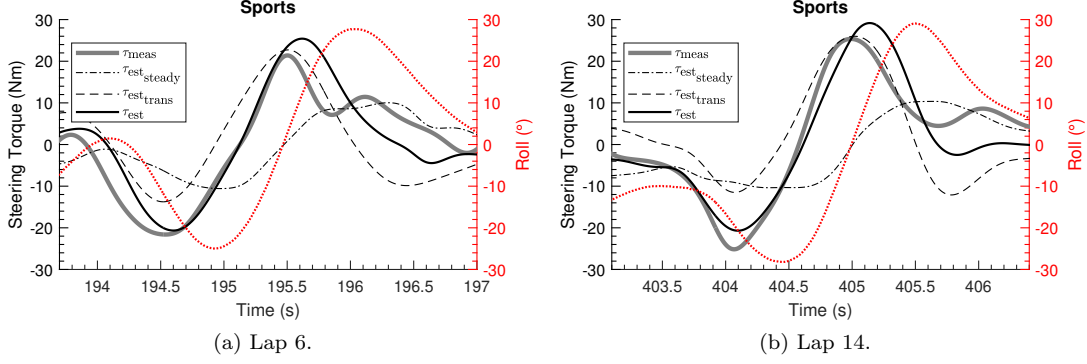


Figure 10. Measured (solid, grey line) and estimated (solid, black line) steering torque during a lane change with the sports motorcycle. The steady (dash-dot, black line) and transient (dotted, black line) contributions of the estimated torque are also shown. The dashed, red line indicates the roll.

have different phases, their frequency is similar and can be approximated by:

$$f = \frac{v}{2d}, \quad d = \sqrt{(\Delta x)^2 + (\Delta y)^2}, \quad (20)$$

where Δx and Δy are the lane change effective¹³ transition distance and offset, respectively, so that d approximates the distance travelled. For the lane change considered, $(\Delta y)^2 \ll (\Delta x)^2$ and $d \approx \Delta x$. The ‘two’ at the denominator of the estimated frequency is because, while riding along the transition distance, the signals go from one peak to that having the opposite sign; therefore, this length corresponds to half the period.

Figure 11 shows the amplitude of the transfer function approximating the LCRI as a function of speed and frequency, which are linked by Equation (20) (dashed lines). The index increased at lower speeds ($\lim_{v \rightarrow 0} \text{LCRI}(\omega) = +\infty$) and lower frequencies ($\lim_{\omega \rightarrow 0} \text{LCRI}(\omega) = +\infty$). The three dashed lines are relative to half, equal to and double the distance covered in the lane change considered. For a specific lane change, decreasing the speed decreased the frequency, and both made the index increase. Considering the average speed (between all runs), equal to 11.7 m s^{-1} , the intersection with the 14 m dashed line provided a frequency of 0.41 Hz, and a $1.98 \text{ N rad}^{-1} \text{ s}^2$ LCRI value, higher than the measured one. However, from the GNSS data, the effective lane change distance turned out to be 12.4 m. Using this value, the estimated LCRI becomes $1.79 \text{ N rad}^{-1} \text{ s}^2$, much closer to the measured value. The frequency calculated using this distance was 0.47 Hz. Notice that $\lim_{\omega \rightarrow \infty} \text{LCRI}(\omega) = c_5 = I_{\text{wf}} \cos \varepsilon / R_f$, obtaining the expression used by Cossalter to approximate the LCRI value [6].

3.2. Scooter and touring motorcycle lane change

For each motorcycle in Cossalter’s article [6], the steady-state and transient steering torque signals were calculated with equations (9) and (10) and summed to obtain the total steering torque, which was then compared with that measured.

Figure 12a shows the scooter signals: the estimated torque had approximately the same shape and amplitude as that measured, which anticipated it. The gyroscopic moment alone gave a reasonable description of the total steering torque with a lower

¹³Effective’ means that it is relative to the manoeuvre actually performed. The rider could start and end the manoeuvre sooner or later than indicated by the cones.

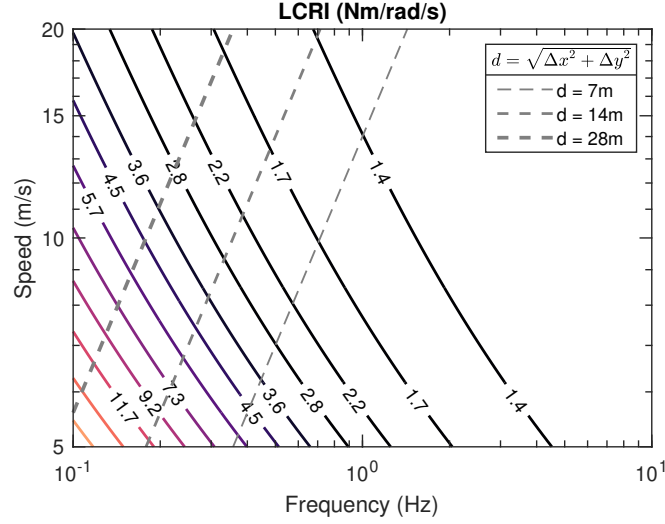


Figure 11. Magnitude of the transfer function approximating the LCRI as a function of speed and frequency for the sports motorcycle. The three dashed lines are relative to half, equal to and double the distance covered in the lane change considered.

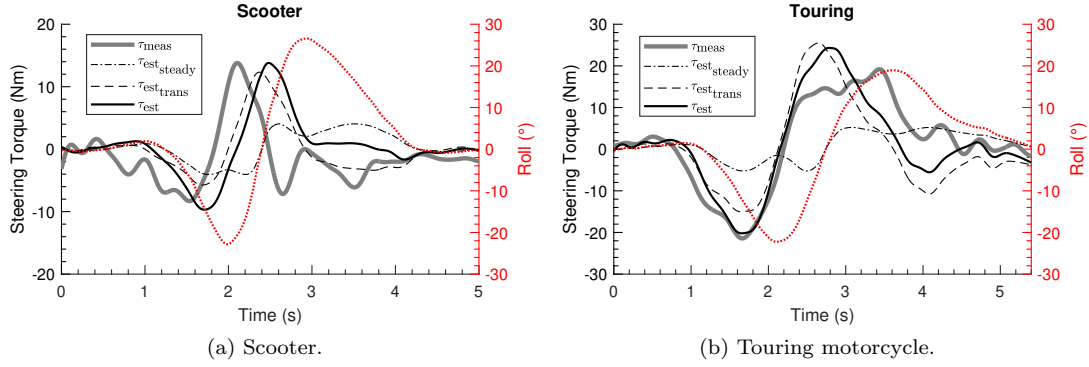


Figure 12. Measured (solid, grey line) and estimated (solid, black line) steering torque during a lane change with the scooter and touring motorcycle. The steady (dash-dot, black line) and transient (dotted, black line) contributions of the estimated torque are also shown. The dashed, red line indicates the roll.

amplitude. Adding τ_{steady} increased the steering torque amplitude, as the linear, dominant term of the steady contribution is $\pi/2$ out of phase to the transient contribution. Figure 12b shows the same signals for the touring motorcycle: again, the transient steering torque component constitutes the bulk of the total steering torque. Adding the steady-state component made the estimated steering torques closer to the measured one, committing a modest error for most of the manoeuvre.

Table 3 reports the LCRI values obtained: the measured LCRI for the touring motorcycle was significantly higher than that for the scooter. For the scooter, using the estimated torque, a $0.97 \text{ N rad}^{-1} \text{ s}^2$ LCRI value was obtained, very close to the measured $1.01 \text{ N rad}^{-1} \text{ s}^2$. The simplified expression by Cossalter underestimated its value by around one-fourth. For the touring motorcycle, the estimated torque provided a $2.29 \text{ N rad}^{-1} \text{ s}^2$ LCRI value, slightly higher than the $2.14 \text{ N rad}^{-1} \text{ s}^2$ value from the measured torque. The value estimated through the simplified formula was close to the measured value and again lower. The values reflect the different masses of the three vehicles, with the sports motorcycle used in this study being in the middle.

Table 3. Lane Change Roll Index calculated using the measured steering torque, the estimated steering torque and through the simplified formula that only considers the transient steering torque, for the scooter and the touring motorcycle.

Motorcycle	LCRI ($\text{N rad}^{-1} \text{s}^2$)		
	Using τ_{meas}	Using τ_{est}	$I_{\text{wff}} \cos \varepsilon / R_f$
Scooter	1.01	0.97	0.75
Touring	2.14	2.29	2.09

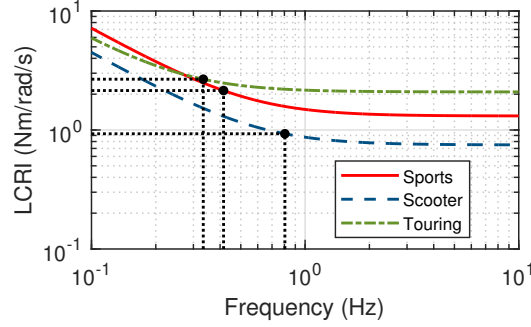


Figure 13. Lane Change Roll Index transfer function for each motorcycle considered in this study. The transfer function is relative to the average speed of the runs depicted in Figures 10b, 12a and 12b, respectively. Frequencies calculated through Equation (20).

3.3. Lane Change Roll Index transfer function comparison

Figure 13 shows the transfer function describing the LCRI for the sports, scooter and touring motorcycles. The transfer functions are relative to the average speed of the runs depicted in Figures 10b, 12a and 12b, respectively. The general trend was the same, with a 20 dB per decade slope on the left and an asymptotic value for higher frequencies, but some quantitative differences emerged. The scooter was the most manoeuvrable at all frequencies. The sports motorcycle was less manoeuvrable, with a 60% higher LCRI at 0.1 Hz and a 75% higher right asymptote. The transfer function predicted the touring motorcycle to require slightly less steering torque at lower frequencies than the sports motorcycle but significantly more at higher frequencies. The frequency calculated through Equation (20) is also shown in the plot for each motorcycle, as the lane change geometry was chosen to be appropriate for the vehicle class.

4. Discussion

Results globally showed a good agreement between the measured and estimated steering torque. Consequently, the simplifying hypotheses discussed in Subsection 2.5 proved valid, introducing a reasonable error.

Figure 4 showed that the estimated steering torque signal had dynamics and amplitude similar to that measured for the various manoeuvres considered. Figure 5 showed an alternative and more general view, albeit limited to the steady-state domain. The modest difference between the estimated torque and that obtained through regression implied that the motorcycle parameters used agree with those obtained through the best-fit of the measured torque when using the proposed formulation. The speed de-

pendency was lost at higher speeds: the same lateral acceleration is obtained with a small steering angle that cannot influence the resulting steady-state steering torque, which becomes uniquely determined by the lateral acceleration.

Subsection 3.1.2 presents the roll-to-torque transfer function $H_{\phi \rightarrow \tau}(s)$: as Figure 6 showed, its static value is the absolute minimum, maintained in a wide frequency range. This result agrees with what Lot shows [12, p. 306]. Therefore manoeuvrability is highest at lower frequencies when considering the roll as the motorcycle response, independently of motorcycle parameters. Beyond the frequency of the zero, the transfer function amplitude increases with a 20 dB per decade slope: the motorcycle becomes progressively less manoeuvrable. The frequency of the zero for a specific motorcycle is a function of both the speed and the equilibrium roll (Figure 8b). Although the transient term influences the amplitude starting from a frequency between 0.1 Hz and 1 Hz, its influence on the phase starts from a decade earlier. Consequently, a slow, transient manoeuvre should not require more steering torque than a steady corner having the same roll, but the transient, gyroscopic effect would induce a delayed roll response. An increased steering input required for the same roll amplitude and a higher response delay are indicators of worse handling [2].

$H_{\phi \rightarrow \tau}(s)$ is a single zero, which is negative for low to moderate roll angle values, so the torque-to-roll transfer function would have a single, negative pole. The poles directly define the homogeneous response components. As the only pole is real and negative, this transfer function would predict a stable, non-oscillatory free evolution of the roll angle. Moreover, as the pole (or zero) becomes more negative at lower speeds (Figure 8b), it would predict higher hands-off stability when travelling slowly. This conclusion clearly contrasts with simple models for a two-wheeled vehicle [16] and experimental evidence [17]. The reason for this apparent contradiction is that all the equations presented follow the initial hypothesis that the derivative of the angular momentum of the front frame is negligible. Under this hypothesis, the steering torque applied by the rider balances all the other torques acting on the steering: in a hands-off situation, this assumption is clearly no longer valid, manifesting as rapid movements of the steering assembly. So, the proposed transfer functions inform about the forced response, but are not sufficient for the homogeneous response.

The influence of the manoeuvre and motorcycle parameters reflects on the transfer function. For manoeuvres around small roll values, Equation (17) becomes:

$$H_{\phi \rightarrow \tau} \big|_{\phi_0 \approx 0}(s) \approx c_1 g + c_3 \frac{g}{v^2} + c_5 v s, \quad (21)$$

which, except for very low speeds, is equivalent to:

$$H_{\phi \rightarrow \tau} \big|_{\phi_0 \approx 0, v \gg 0}(s) \approx c_1 g + c_5 v s, \quad (22)$$

as shown by the static gain of Figure 7a becoming constant with speed over a specific speed value. Consequently, in many common driving conditions (e.g. highway lane change), the transfer function describing the manoeuvrability has a static term, which takes into account the twisting moment and the gyroscopic moment of the front wheel linked to the yaw rate, and a dynamic term linked to the gyroscopic moment due to the roll rate. While the former is constant, the latter is proportional to speed in addition to the manoeuvre frequency: at higher speeds, the transient term is perceived starting from lower frequencies, as confirmed by Figure 7a. For very high speeds, the transient, gyroscopic term would make the most of the transfer function amplitude even

at lower frequencies, defining the motorcycle manoeuvrability. This fact could explain why the rider acts as a position servo at low speeds and a torque servo at higher speeds [18]: at lower speeds, the zero is higher than the rider input frequencies, so the roll response does not depend on how rapidly the torque is applied, and consequently how fast the steering turns. The opposite holds at higher speeds, with the input frequency influencing the torque to be applied. For motorcycles frequently used at high speeds and frequencies, e.g. for track riding, reducing the front-wheel spin inertia is crucial to improve manoeuvrability, while intervening on other parameters should have more limited effects. Lower spin inertia would also reduce the influence of speed and frequency on the required torque, possibly making motorcycle behaviour more intuitive.

The sensitivity analysis concerning the design parameters shows that the front nondimensionalised twisting stiffness, its vertical load and the normal trail only influence the steady behaviour, while the front-wheel spin inertia and the caster influence the manoeuvrability in the whole frequency domain; however, the latter seemed to have a marginal effect. The twisting moment is misaligning, so increasing the twisting stiffness made the torque required to the rider even more aligning, increasing the steady torque. This sign is coherent with the results of the much more complex motorcycle model by Cossalter [13]. The same was true for the front tyre load and the normal trail, in agreement with the model above. Therefore, increasing the twisting stiffness reduces manoeuvrability during gradual manoeuvres but leads to a less delayed response at medium frequencies. Notice that a front load increase also increases the *dimensional* twisting stiffness. If the caster increased, the steady-state amplitude reduced; Cossalter [13] confirms this but shows a much more significant impact. That study considers a motorcycle in a curve with a 5 m s^{-2} lateral acceleration, while Figure 9d is relative to $\phi_0 = 0$, so it does not consider some terms of Equation (17) and most of the caster influence with them. Lastly, a front-wheel spin inertia increase increases both (yaw- and roll-related) gyroscopic torques, slightly increasing manoeuvrability at lower frequencies while making the motorcycle significantly more demanding to steer at higher frequencies, leading to more frequency-sensitive manoeuvrability. Therefore, one specific frequency exists where this parameter change does not influence the amplitude while still impacting the phase.

Table 2 confirms the robustness of the LCRI: the measured value had a 0.083 coefficient of variation, much smaller than the variability of the individual signals forming the index. While the input steering torque and the output roll and roll rate are subject to variation, these are linked by the physical behaviour of the motorcycle. The mean LCRI value was approximately the same whether the measured or the estimated torque was used, whose estimation error was limited even under transient conditions. The approximate formula proposed by Cossalter, although easy to calculate, underestimates the index value. The transfer function approximating the LCRI (Equation (19)) shows why: $\lim_{\omega \rightarrow \infty} \text{LCRI} = \lim_{v \rightarrow \infty} \text{LCRI} = c_5 = I_{\text{wf}} \cos \varepsilon / R_f$. Consequently, the approximated expression is only valid for high speed or frequencies: as shown by Figure 11, the transfer function has a minimum in the upper-right corner, taking on greater values elsewhere. The higher the speed, the lower the minimum frequency required to avoid significant estimation errors. At lower frequencies, especially if the speed is also low, as in the case of these lane changes, the stationary term increases the steering torque required and, therefore, the index value¹⁴. Consequently, the simplified expression by Cossalter gives a lower limit for the LCRI. In fact, in the original article [6], the

¹⁴For very low frequencies, the index value approaches infinity because the steering torque tends to the steady-state value while the roll rate approaches zero. Using roll as the motorcycle response is more appropriate to assess low-frequency manoeuvrability, as in the roll-to-torque transfer function.

measured LCRI matches or exceeds that obtained through the simplified formula for various motorcycle classes.

Figures 10,12 showed that the steering torque signal could be estimated for motorcycles of differing characteristics performing lane changes with vastly different geometries. The transient, gyroscopic term underestimated the peak values, and the total estimated torque was closer to that measured in the entry and cornering phase than in the exit phase. Adding the steady-state term postponed the peaks, especially the second one: in fact, the dominant, linear steady contribution is delayed $\pi/2$ compared to the transient term. For the sports motorcycle, $\tau_{\text{steady}}(t)$ had an approximately-sinusoidal trend: the second-degree steady term had a limited influence, and the steady contribution remained clearly counter-steering. Conversely, for the scooter and touring motorcycle, $\tau_{\text{steady}}(t)$ has a hump when the roll is highest. Therefore, the sports motorcycle did not reach the $a_y|_{\tau=\tau_{\text{max}}}$ lateral acceleration value. Instead, the other two motorcycles exceeded it, without reaching the $a_y|_{\tau=0}$ value: the steady-state torque remained counter-steering throughout the manoeuvre. The accuracy of the reconstructed steering torque signal is somewhat higher in Figure 10 than Figure 12, partly due to the limited knowledge of the parameters of the motorcycles found in the literature.

Lastly, Figure 13 compared the predicted manoeuvrability of the three motorcycles. The scooter requires relatively small torque inputs at all frequencies. The lower load on the front tyre reduces most steady-state torque contributions, and the narrow front tyre further reduces the misaligning twisting torque. The small front tyre has a lower mass and radius of gyration, reducing the high-frequency torque too. The transfer function for the touring motorcycle predicts better low-frequency manoeuvrability than the sports motorcycle, despite the higher mass and size. The higher front tyre spin inertia and normal trail reduce the stationary steering torque (Figures 9b,9e). However, the higher spin inertia increases the steering torque required at higher frequencies (Figure 9b), making quick manoeuvres more demanding than for the sports motorcycle. These transfer functions were relative to the speed of the specific manoeuvre, the effect of which overlaps with the intrinsic characteristics of the vehicles. However, the three manoeuvres were performed at similar speeds, so this effect is tiny. The frequency of each manoeuvre was slightly lower than the value over which the LCRI reaches its asymptotic value: this explains the underestimation made by the simplified formula by Cossalter and shows that the lane change geometry was chosen appropriately for each vehicle's class¹⁵.

Future development could focus on extending the experimental dataset. For example, it may include a comparison of the estimated and the measured torque for faster manoeuvres, as this work considered low and medium-speed manoeuvres; this would allow testing the accuracy of the steering torque map shown in Figure 5a on a broader speed range. Peculiar motorcycle classes, such as supersport or off-road motorcycles, could be added to validate the approach further. The estimation equations could be generalised to cover combined dynamics conditions. This could be done by adding the load transfer, estimated from the longitudinal acceleration signal, to the front tyre static load in Equation (9). The brake-steering torque could be estimated from the front braking force through the front tyre radius, caster angle and instantaneous roll angle. Lastly, the correlation between the manoeuvrability estimated by a transfer function for different manoeuvres and motorcycles and the subjective handling perceived by

¹⁵For example, if the manoeuvres of the scooter and the touring motorcycle were inverted, the transfer function of the former would be evaluated at a relatively low frequency with a significant influence of the steady term. On the contrary, the latter would be excited at a frequency such that the asymptotic behaviour would be achieved, provided the rider can perform such a tight manoeuvre.

the rider during the corresponding run could be investigated to determine whether the approach and the results shown in this paper could also predict riding feel.

5. Conclusion

This work proposed a motorcycle steering torque estimation methodology based on a simplified steering assembly model. The model only requires a limited set of readily available or easily measurable motorcycle parameters; this also allowed the estimation of the steering torque of motorcycles from other datasets. The estimation equation was employed to define transfer functions describing motorcycle manoeuvrability: the influence of the manoeuvre and motorcycle parameters was shown and discussed. The results extend what was found by Cossalter regarding the lane change manoeuvre: they confirm that estimating the Lane Change Roll Index by only considering the gyroscopic torque is feasible, but only as long as the manoeuvre frequency is sufficiently high, with the frequency threshold dependent on the speed and motorcycle properties. If this threshold is not exceeded, the transfer function for the LCRI proposed in this article provides a more accurate value.

This work allows recreating the steering torque signal for new and pre-existing datasets for which the torque measurement was not feasible or of interest, describing the rider effort required during previous tests. The signals required¹⁶ for estimation are commonly measured in experimental tests. The simplicity of the estimation equation reduces the computational cost compared to more complex models, potentially making it an ideal candidate for developing steering assistance systems.

Data availability statement

The data that support the findings of this study are available from the corresponding author, Bartolozzi M, upon reasonable request.

Disclosure statement

No potential conflict of interest was reported by the author(s).

References

- [1] Weir DH, Zellner JW. Lateral-directional motorcycle dynamics and rider control. Publication of: Society of Automotive Engineers. 1978;.
- [2] Biral F, Bortoluzzi D, Cossalter V, et al. Experimental study of motorcycle transfer functions for evaluating handling. *Vehicle System Dynamics*. 2003;39:1 – 25.
- [3] A dictionary of terms for the dynamics and handling of single track vehicle. Society of Automotive Engineers; 2019. Standard.
- [4] Koch J. Experimentelle und analytische untersuchungen des motorrad-fahrer-systems. *VDI-Z*. 1980 08;122 (1980).
- [5] Cossalter V, Lot R, Massaro M, et al. Investigation of motorcycle steering torque components. *AIP Conference Proceedings*. 2011 10;1394:35–46.

¹⁶The speed and the roll angle or, alternatively, the lateral acceleration or yaw rate and the roll rate.

Table A1. Values of the parameters of the three motorcycles considered in this study.

Motorcycle Model	Parameter						
	k_{tf} (m rad ⁻¹)	I_{wf} (kg m ²)	F_{zf} (N)	ε (rad)	a_n (m)	R_f (m)	l (m)
Sports	0.035	0.43	1430	0.424	0.085	0.300	1.52
Scooter	0.025	0.22	1060	0.463	0.115	0.250	1.38
Touring	0.027	0.75	2080	0.475	0.135	0.320	1.64

- [6] Cossalter V, Sadauckas J. Elaboration and quantitative assessment of manoeuvrability for motorcycle lane change. *Vehicle System Dynamics*. 2006;44(12):903–920.
- [7] Cossalter V, Lot R, Peretto M. Steady turning of motorcycles. *Proceedings of The Institution of Mechanical Engineers Part D-journal of Automobile Engineering - PROC INST MECH ENG D-J AUTO*. 2007 11;221:1343–1356.
- [8] Sharp RS. The stability and control of motorcycles. *Archive: Journal of Mechanical Engineering Science 1959-1982 (vols 1-23)*. 1971;13:316–329.
- [9] Cossalter V, Lot R. A motorcycle multi-body model for real time simulations based on the natural coordinates approach. *Vehicle System Dynamics*. 2002 06;00.
- [10] Road vehicles - vehicle dynamics and road-holding ability - vocabulary. *International Organization for Standardization*; 2011. Standard.
- [11] Massaro M, Cole D. Neuromuscular-steering dynamics: Motorcycle riders vs. car drivers. In: *Dynamic Systems and Control Conference*; 10; 2012. p. 217–224.
- [12] Lot R, Sadauckas J. *Motorcycle design*. 1st ed. Lulu.com; 2021.
- [13] Cossalter V, Doria A, Lot R. Steady turning of two-wheeled vehicles. *Vehicle System Dynamics - VEH SYST DYN*. 1999 03;31:157–181.
- [14] Cossalter V, Lot R, Maggio F. The influence of tire properties on the stability of a motorcycle in straight running and curves. In: *SAE Technical Papers*; may. SAE International; 2002.
- [15] Cossalter V. *Motorcycle dynamics*. 2nd ed. Lulu.com; 2006.
- [16] Schwab AL, Meijaard JP. A review on bicycle dynamics and rider control. *Vehicle System Dynamics*. 2013;51(7):1059–1090.
- [17] Singhania S, Kageyama I, Karanam VM. Study on low-speed stability of a motorcycle. *Applied Sciences*. 2019;9(11).
- [18] Lenkeit J. A servo rider for the automatic and remote path control of a motorcycle. *SAE transactions*. 1995;104:367–372.
- [19] Cossalter V, Doria A. The relation between contact patch geometry and the mechanical properties of motorcycle tyres. *Vehicle System Dynamics*. 2005;43(sup1):156–164.

Appendix A. Motorcycle parameters

Table A1 contains the values of each parameter required to estimate the steering torque for each motorcycle considered in this study. For the sports motorcycle, the caster, normal trail, front tyre radius and wheelbase were obtained from the OEM spec sheet. The front-wheel spin inertia was set equal to the value of another motorcycle of similar characteristics; the nondimensionalised twisting stiffness was set equal to the mean of the values relative to front tyres having the same size and similar characteristics, from the available literature [19]. Most of the values relative to the other two vehicles were taken from the original paper [6]; those not available in the article were taken from motorcycles of similar characteristics.

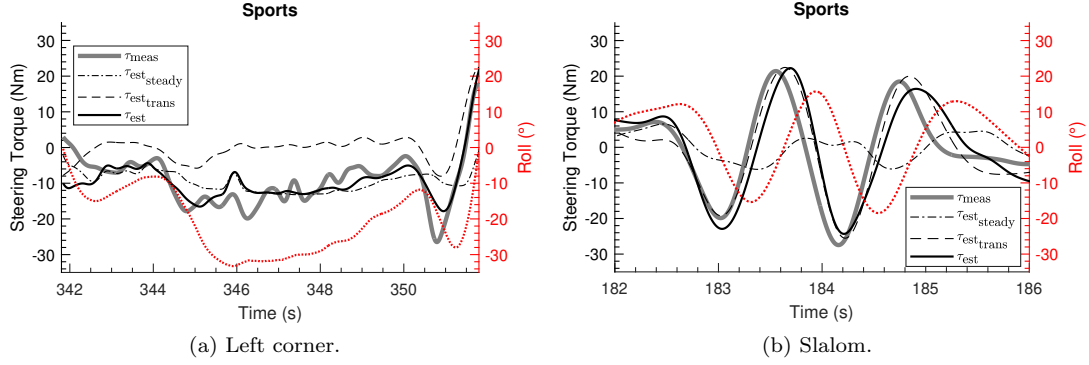


Figure B1. Measured (solid, grey line) and estimated (solid, black line) steering torque during a left corner and slalom with the sports motorcycle. The steady (dash-dot, black line) and transient (dotted, black line) contributions of the estimated torque are also shown. The dashed, red line indicates the roll.

Appendix B. Left corner and slalom manoeuvres

Figure B1 insights the estimation of steering torque during a left-hand bend (Figure B1a) and a slalom (Figure B1b).

For the corner, the roll increased, reaching the maximum around 346s, which is maintained for around 2s and then reduced again to zero. Around 351s, the rider applied a correction to align the motorcycle for the successive lane change. The measured steering torque monotonically increased with the motorcycle roll; the estimated torque agreed with the measured one. For this manoeuvre, the steady-state contribution made up most of the estimated torque: the low frequency of the manoeuvre limited the effect of the roll-related gyroscopic torque. Still, in the most abrupt sections of this manoeuvre (345s, 351s), the roll rate was significant, and considering the roll-related gyroscopic torque made the estimated torque much closer to the measured one. Lastly, while the steady component of the estimated torque is in phase with the roll, both the measured and the total estimated torque are anticipated slightly due to the roll-induced gyroscopic torque.

The estimated and measured steering torque also agreed during the slalom. The peaks had similar values, except for the first part of the manoeuvre when the estimated torque tended to lag the measured one.